JOURNAL OF APPLIED ELECTROCHEMISTRY **10** (1980) 127–141

# *Studies concerning charged nickel hydroxide electrodes. II. Thermodynamic considerations of the reversible potentials*

R. BARNARD, C. F. RANDELL, F. L. TYE

*Berec Group Limited, Group Technical Centre, St Ann's Road, London N15, UK*

Received 30 March 1979

In this paper the thermodynamics of mixing are applied to account for the independence of the discharge potential of the nickel hydroxide electrode as a function of nickel oxidation state. The constant potential region is considered to arise from the formation of a pair of co-existing solid solutions having a composition predetermined by the magnitude of the interactions between the oxidized and reduced species. From considerations of the excess-energy terms, it can be shown for a symmetrical potential/composition profile, that the constant potential region is identical with the standard potential $E_0$. The influence of asymmetry on the changes in $E_0$ are discussed. Consideration has also been made of the influence of dissociation of oxidized and/or reduced species on the potential determining equations. The removal of n-type defects from the nickel(II)-rich phase on discharge is considered to be responsible for the observed secondary discharge plateau at potentials ~ 300 mV more cathodic than normal. This non-equilibrium behaviour can be explained in terms of a mixed pn-semiconducting material.

**List of symbols**

| | | | |
|---|---|---|---|
| $E$ | electrode potential at constant pH (V) | $G_R$ | free energy of reaction (J mole$^{-1}$) |
| $E_0$ | standard electrode potential (V) | $G_I$ | free energy of mixing under ideality (J mole$^{-1}$) |
| $R$ | the gas constant (J K$^{-1}$ mole$^{-1}$) | $G_E$ | excess free energy (J mole$^{-1}$) |
| $F$ | the Faraday constant (C g-equiv$^{-1}$) | $A$, $A_I$ and $B_I$ | interaction energy parameters (J mole$^{-1}$) |
| $T$ | the absolute temperature (K) | $x_u$ | mole fraction of y in co-existing phase u |
| $a_{H^+}$ | proton activity in the electrolyte | $x_v$ | mole fraction of y in co-existing phase v |
| $a_z$ | activity of oxidized species z | $\gamma_y$ | activity coefficient of undissociated reduced species y |
| $a_y$ | activity of reduced species y | $\gamma_z$ | activity coefficient of undissociated oxidized species z |
| $\mu_{H^+}$ | chemical potential of the proton | $\gamma_y^{\pm}$ | mean ionic activity coefficient of y |
| $\mu_e$ | chemical potential of the electron | $\gamma_z^{\pm}$ | mean ionic activity coefficient of z |
| $\mu_z^0$ | standard chemical potential of species z | $\gamma_y^u$ | activity coefficient of y in phase u |
| $\mu_z$ | chemical potential of species z | $\gamma_z^u$ | activity coefficient of z in phase u |
| $\mu_y^0$ | standard chemical potential of species y | $\gamma_y^v$ | activity coefficient of y in phase v |
| $\mu_y$ | chemical potential of species y | $\gamma_z^v$ | activity coefficient of z in phase v |
| $\mu_{H,e}$ | chemical potential of the proton/electron pair | $I$ | current (A) |
| $x_y$ or $x$ | mole fraction of reduced species y | S | cross-sectional area (cm$^2$) |
| $x_z$ | mole fraction of oxidized species z | L | conductor length (cm) |
| $G_M$ | total free energy of mixing (J mole$^{-1}$) | | |

0021–891X/80/010127–15$03.50/0 

| | |
|---|---|
| $\sigma_e^0$ | specific conductivity of the electron ($\Omega^{-1}$ cm$^{-1}$) |
| $\sigma_h^0$ | specific conductivity of the hole ($\Omega^{-1}$ cm$^{-1}$) |
| $\eta$ | potential difference across conductor (V) |
| $\psi$ | proton–electron spatial correlation coefficient |
| $N$ | number of $Ni^{3+}$ ions injected into $Ni(OH)_2$ |
| $N_0$ | Avagadro's number |

## 1. Introduction

Oxidation of $Ni(OH)_2$ to the higher oxides occurs exclusively in the solid state [1]. The very low solubility of $Ni^{2+}$ in alkaline media precludes soluble intermediates. Whether or not the oxidation process takes place 'homogeneously' is open to dispute, certainly X-ray diffraction, [2–5] and visual evidence [6–8] are inconclusive in this respect. If the oxidation and reduction processes took place within the same phase the reversible potential would be expected to vary as a function of the degree of oxidation of the electrode because of the changing activities of the species within the solid phase [9]. Whilst this may be true [10] during the initial stages of oxidation (up to ~ 10%) several investigators [1, 10, 11] have shown, for essentially $\beta$-phase starting materials, that for the greater part of the oxidation process the e.m.f. is independent of the degree of oxidation of the electrode. Recent measurements [11] have confirmed previous observations and have shown that the $\alpha$-$Ni(OH)_2$/$\gamma$-NiOOH system behaves similarly. In order to obtain reliable potential data [11] considerable care must be taken to avoid cross-contamination between the various activated and de-activated phases.

I.r. spectroscopic measurements [12–16] have shown that $\beta$-$Ni(OH)_2$ gives rise to a sharp band at 3650 cm$^{-1}$ characteristic of 'free' non-hydrogen bonded $OH^-$ groups. On charging this band progressively disappears because of the development of a hydrogen bonded structure. This is apparent also from a band for the charged active material at 580 cm$^{-1}$ indicating motion of the hydrogen bonded linkages relative to the nickel sites. Because on discharge of $\beta$- or $\gamma$-NiOOH the sharp OH band reappears, this has been taken to support the presence of discrete $\beta$-$Ni(OH)_2$, i.e. a heterogeneous reduction process. If the discharge involved formation of extensive solid solutions then solvent–solute interactions should be seen and this would be manifest in either a shift or a broadening of the 3650 cm$^{-1}$ band and additional combination bands.

The purpose of the present paper is to provide further understanding of the nature of the processes which cause the independency of reversible potential with degree of oxidation over wide limits for the nickel hydroxide electrode.

## 2. General considerations

The operation of metal oxide cathodes can be described by the general equation

$$z + nH^+ + ne \rightarrow y \qquad (1)$$

where for the present case z is NiOOH and y is $Ni(OH)_2$ and the number of electrons transferred $n$ is 1. In this interpretation the function, in the cathodic reaction, of the metal hydroxide (oxide) is to provide a sink for electrons coming from the outer circuit and protons from the electrolyte. A general Nernst relationship for Equation 1 can be written for the potential $E^1$ using hydrogen as the reference electrode as:

$$E^1 = E_0 + \frac{RT}{F} \ln (a_z/a_y) + \frac{RT}{F} \ln a_{H^+} \qquad (2)$$

where $E_0$ is the standard potential. $a_z$, $a_y$ and $a_{H^+}$ are the activities of z, y and $H^+$ respectively, $R$ is the gas constant, $F$, Faraday's constant and $T$ the absolute temperature. At constant pH Equation 2 reduces to

$$E = E_0 + \frac{RT}{F} \ln (a_z/a_y) \qquad (3)$$

where $E = (E^1 - \text{constant})$.

In simple treatments the system is considered to behave homogeneously and in the ideal case the activity terms are replaced by mole fractions of species z and y, respectively. Clearly such a simplification is untenable where the e.m.f. remains invariant over a wide range of composition. The problem resolves into one of deciding on expressions to be used for the activity terms for y and z in Equation 3.

It will be shown that the change (or invariance)

of potential with degree of oxidation can be considered as resulting from the free energy changes which take place as a consequence of mixing of the oxidized and reduced species in the solid phase. In the operation of metal oxide/hydroxide electrodes at ambient temperature the mixing occurs indirectly via the movement of protons and electrons. For thermodynamic purposes these processes must be regarded as occuring sufficiently rapidly so that equilibrium can be maintained. Recently Atlung [17] has discussed the useful concept of the chemical potential of the proton–electron pair $\mu_{H,e}$. Accordingly the electrode potential can be shown to be given by:

$$E = -\frac{1}{F}(\mu_{H^+} + \mu_e) = \frac{1}{F}(\mu_z - \mu_y). \quad (4)$$

Thus whether the electrode is considered from the standpoint of the movement of proton–electron pairs or the mixing of y and z leads to the same conclusion.

### 3. Thermodynamic considerations of mixtures and the Nernst equation

In order to develop equations to describe the electrode potential as a function of degree of oxidation, thermodynamic considerations of mixtures are required. These have been thoroughly established by the extensive work of Hildebrand [18], and Guggenheim [19]. For the present treatment the oxidized and reduced species will be treated as undissociated components, analogous to mixtures of non-ionic organic liquids. Later, in Section 9, the influence of dissociation will be considered separately.

The mixing model is based on the considerations of the changes in free energy on mixing two species y and z in a solid solution from $x_y$ of 0 to 1 where $x_y$ is the mole fraction of y. If the system is assumed to be ideal then the total free-energy $G_M$ is given by the sum of the total free energy of reaction $G_R$ and the free energy due to mixing $G_I$. For most real systems interactions exist between the molecules or ions in the solid and a third correction term for the so-called excess energy $G_E$ must be added. The excess energy can show either positive or negative deviations from ideal behaviour. It can be shown [18] that the various quantities are given by the expressions as follows:

$$G_R = (1-x_y)\mu_z^0 + x_y\mu_y^0 \quad (5)$$

$$G_I = RT[(1-x_y)\ln(1-x_y) + x_y \ln x_y] \quad (6)$$

$$G_E = RT[(1-x_y)\ln\gamma_z + x_y \ln\gamma_y] \quad (7)$$

where $\mu_z^0$ and $\mu_y^0$ are the standard chemical potentials of z and y respectively and $\gamma_z$ and $\gamma_y$ are the activity coefficients of z and y respectively, noting that;

$$x_y + x_z = 1. \quad (8)$$

Expressions for $\gamma_y$ and $\gamma_z$ have been proposed by Margules and also Van Laar [17] and in the simplest case (see also Section 5) reduce to:

$$\ln\gamma_y = \frac{A}{RT}(1-x_y^2) \quad (9)$$

$$\ln\gamma_z = \frac{A}{RT}x_y^2 \quad (10)$$

where $A$ is a constant. Similar expressions can be derived from the statistical mechanical methods of Guggenheim [19]. Since

$$G_M = G_R + G_I + G_E \quad (11)$$

and substituting Equations 9 and 10 into Equation 7 this leads to:

$$G_M = (1-x_y)\mu_z^0 + x_y\mu_y^0 + RT[(1-x_y)\ln(1-x_y) + x_y \ln x_y] + RT\left[\frac{A}{RT}(x_y - x_y^2)\right]. \quad (12)$$

On differentiation of Equation 12 and putting $x_y = x$

$$\frac{dG_M}{dx} = [\mu_y^0 - \mu_z^0] + RT\ln\frac{x}{(1-x)} + RT\frac{A}{RT}(1-2x) \quad (13)$$

since

$$\frac{dG_M}{dx} = -nFE \quad (14)$$

$$E = \left[\frac{(\mu_z^0 - \mu_y^0)}{nF}\right] + \frac{RT}{nF}\left[\ln\frac{(1-x)}{x}\right] + \frac{RT}{nF}\left[\frac{A}{RT}(2x-1)\right]. \quad (15)$$

Equation 15 is a form of the Nernst equation which takes into account departure of the electrode from ideal behaviour. Equation 13 can be used further to determine the conditions under which a homogeneous solid solution of y and z would separate into co-existing solid-solution phases. On differentiation of Equation 13

$$\frac{d^2G_M}{dx^2} = RT\left[\frac{1}{x(1-x)} - \frac{2A}{RT}\right]. \quad (16)$$

It is clear that Equation 16 can take up negative values for certain $A/RT$. If a two-component mixture of y and z is to remain thermodynamically stable then $(d^2G_M/dx^2) \geqslant 0$. If $(d^2G_M/dx^2)$ is negative the mixture can no longer exist as a single phase [18]. Because for the simple case in point the $G_E$ function (Equation 7) is symmetrical, the critical point for phase separation is found when $(d^2G_M/dx^2) = 0$ and $x = 0{\cdot}5$. On substitution of these values into Equation 16 clearly $A/RT = 2$. Thus when $A > 2RT$ phase separation must occur. This conclusion is drawn by Guggenheim [19].

If separation occurs into phases u and v there exist mole fractions $x_u$ and $x_v$ such that:

$$\mu_y(T, x_u) = \mu_y(T, x_v) \quad (17)$$

and

$$\mu_z(T, x_u) = \mu_z(T, x_v) \quad (18)$$

but

$$\mu_z^0(T) + RT\ln(1-x_u)\gamma_z^u = \mu_z^0(T) + RT\ln(1-x_v)\gamma_z^v \quad (19)$$

and

$$\mu_y^0(T) + RT\ln x_u\gamma_y^u = \mu_y^0(T) + RT\ln x_v\gamma_y^v. \quad (20)$$

Substituting the expressions for $\gamma_y$ and $\gamma_z$ (Equations 9 and 10) in Equations 19 and 20 gives

$$\ln(1-x_u) + \frac{A}{RT}x_u^2 = \ln(1-x_v) + \frac{A}{RT}x_v^2 \quad (21)$$

and

$$\ln x_u + \frac{A}{RT}(1-x_u)^2 = \ln x_v + \frac{A}{RT}(1-x_v)^2 \quad (22)$$

hence

$$\ln\frac{x_u}{x_v} = \frac{A}{RT}\left[(1-x_v)^2 - (1-x_u)^2\right]. \quad (23)$$

If Equations 9 and 10 are symmetrical with

$$x_v + x_u = 1 \quad (24)$$

then Equation 23 reduces to:

$$\frac{A}{RT} = \frac{\ln[x_u/(1-x_u)]}{(2x_u - 1)}. \quad (25)$$

Equation 25 can be used to evaluate the value of $A/RT$ when the composition of the separating phases u and v are known. A direct consequence of the system separating into co-existing phases u and v is that the potential remains constant whilst these two phases are present. Furthermore all solid solutions which separate between the limits defined by Equations 24 and 25 are mixtures of the two co-existing phases having defined composition.

The Nernst relationships for the two phases can be written as follows:
for phase u

$$E = \frac{(\mu_z^0 - \mu_y^0)}{nF} + \frac{RT}{nF}\ln\frac{(1-x_u)\gamma_z^u}{(x_u\gamma_y^u)} \quad (26)$$

for phase v

$$E = \frac{(\mu_z^0 - \mu_y^0)}{nF} + \frac{RT}{nF}\ln\frac{x_u\gamma_z^v}{(1-x_u)\gamma_y^v}. \quad (27)$$

Clearly from Equations 26 and 27

$$\frac{(1-x_u)\gamma_z^u}{x_u\gamma_y^u} = \frac{x_u\gamma_z^v}{(1-x_u)\gamma_y^v} \quad (28)$$

From Equations 9 and 10 further observations regarding phases u and v may be drawn thus

$$\gamma_z^u = \exp\left[\frac{A}{RT}(1-x_u)^2\right] \quad (29)$$

$$\gamma_z^v = \exp\left[\frac{A}{RT}x_u^2\right] \quad (30)$$

$$\gamma_y^v = \exp\left[\frac{A}{RT}x_u^2\right] \quad (31)$$

$$\gamma_y^v = \exp\left[\frac{A}{RT}(1-x_u)^2\right] \quad (32)$$

hence

$$\gamma_z^v = \gamma_y^u \quad (33)$$

and

$$\gamma_z^u = \gamma_y^v. \quad (34)$$

Thus Equation 28 can be rewritten as:

$$\frac{(1-x_u)\gamma_z^u}{x_u\gamma_y^u} = \frac{x_u\gamma_y^u}{(1-x_u)\gamma_z^u} \quad (35)$$

hence

$$\frac{(1-x_u)\gamma_z^u}{x_u\gamma_y^u} = 1 \quad (36)$$

so that $$E = \frac{(\mu_z^0 - \mu_y^0)}{nF} = E_0. \qquad (37)$$

This clearly shows that the constant potential defined by Equations 26 and 27 is in fact identical with $E_0$. It should be emphasized that this is only true if the $G_E$ function is symmetrical. However, it will be shown that very large levels of asymmetry are needed to shift the constant potential from the $E_0$ value. Equation 36 shows that although the ratio of activity terms is unity, the activities of the separate components are not unity.

Fig. 1 shows plots of Equation 15 for various values of $A/RT$. The curve for $A/RT = 0$ represents 'ideal' behaviour and corresponds to the simplified Nernst equation where mole-fractions are used to replace the activity terms. In this case no interactions are present between the oxidized and reduced species and the system obeys Raoult's law. Values of $A/RT$ of 1 and $-1$ depict respectively positive and negative deviations from ideality. The curve with $A/RT = 2$ is a special case representing the borderline between a single-phase and a two-phase system. When $A/RT$ becomes 3 phase separation has taken place with $x_u = 0{\cdot}07$

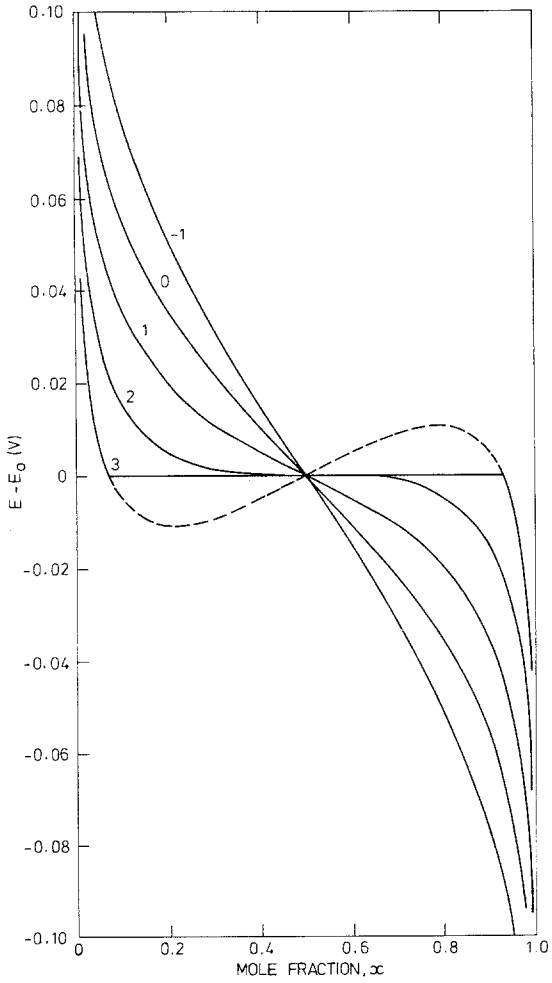


Fig. 1. Plots of $(E - E_0)$ versus $x$ using $E - E_0 = (RT/nF)$ [ln $(1-x)/x + (A/RT)(2x-1)$] for various values of $A/RT$.

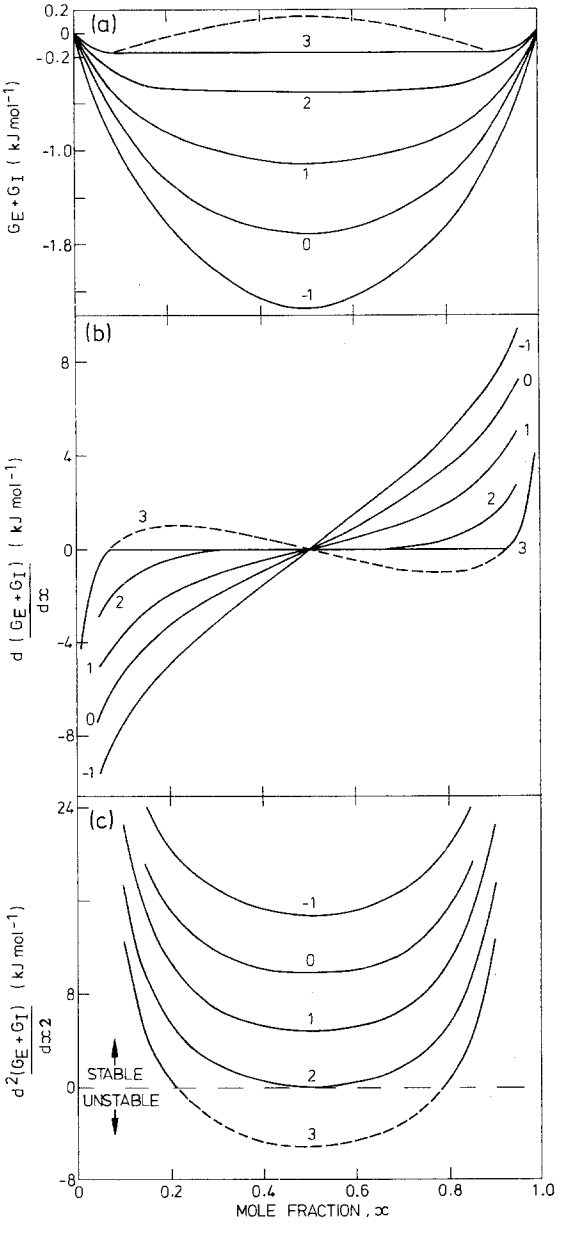


Fig. 2. Plots of $(G_E + G_I)$, $d(G_E + G_I)/dx$ and $d^2(G_E + G_I)/dx^2$ as a function of $x$ for various values of $A/RT$.

and $x_v = 0{\cdot}93$, and the potential remains constant at $E_0$ between these composition limits. The parts of the curve given in Fig. 1 for $A/RT = 3$ shown in broken lines represent non-equilibrium behaviour.

Clearly Equation 15 can be used to generate potential–composition profiles for electrodes having undissociated components showing either homogeneous or heterogeneous discharge characteristics. When viewed in this way the differences in electrode behaviour are seen to be consequences of interactions between the oxidized and reduced species present.

It is of interest to consider the variation of the component energies which give rise to the potential–composition behaviour seen in Fig. 1. Neglecting for the present the reaction energy $G_R$, Fig. 2a–c shows respectively $G_E + G_I$, $d(G_E + G_I)/dx$ and $d^2(G_E + G_I)/dx^2$ plotted as a function of $x$. The electrode potential variation is developed as a consequence of the $d(G_E + G_I)/dx$ function (Equation 13), whilst the conditions for equilibrium are established by $d^2(G_E + G_I)/dx^2$ (Equation 16). For example the fact that $A/RT = 2$ is the critical point of phase operation can be seen from Fig. 2c where the minimum occurs at precisely zero. The negative regions for the $d^2(G_E + G_I)/dx^2$ term describe the regions of instability. For the heterogeneous case with $A/RT = 3$, two metastable zones for $x$, from 0·07 to 0·21 and from 0·79 to 0·93 exist corresponding to the maxima and minima (part of the broken lines) in Figs. 1 and 2b. These are thermodynamically allowed regions but under equilibrium conditions not accessible. The negative values of $d^2(G_E + G_I)/dx^2$ correspond to regions of absolute instability.

## 4. Application to the $\beta$-$Ni(OH)_2$/$\beta$-NiOOH electrode

Previous investigations [11, 20] have indicated that it is only the $\gamma$-phase oxidized material which contains $K^+$ ions. This provides a means of estimating the level of $\gamma$-phase contamination in $\beta$-phase oxidation products particularly when X-ray measurements are insensitive at the 20% level. Accordingly it may be deduced that during the oxidation of $\beta$-$Ni(OH)_2$ to $\beta$-NiOOH the process terminates at a mole fraction of nickel hydroxide near $x = 0{\cdot}25$. Beyond this point the potential changes to allow oxidation of $\beta$-NiOOH to $\gamma$-NiOOH to proceed at a significant rate in addition to oxygen evolution. It is thus reasonable to conclude that this point also corresponds to an oxidation limit in the $\beta$-phase systems [11]. In reality the precise limits are still uncertain because the $Ni(OH)_2$ electrode may not change uniformly throughout its bulk, since discrete uncharged $Ni(OH)_2$ may remain uncharged particularly at low states of total charge.

In the absence of further data, values of $x_u$ of 0·25 and $x_v$ of 0·75 will be (arbitrarily) chosen. From Equation 25 $A$ can be deduced as 2·2 $RT$. Fig. 3a shows the variation of the activities of the $Ni(OH)_2$ and NiOOH as a function of $x$. These values have been derived from Equations 9 and 10. Figs. 3b and c show the variation of $(G_E + G_I)$ and $(E - E_0)$ as a function of $x$. Clearly the proposed model will account for the invariance of the e.m.f.–composition curve between mole fractions of nickel hydroxide of 0·25 and 0·75 as observed experimentally [11]. It should be noted, however, that towards the limits of oxidation and reduction the e.m.f. changes sharply with $x$. Fig. 3b demonstrates that the energies giving rise to phase separation are small ($\sim 0{\cdot}4$ kJ mole$^{-1}$).

Conway and co-workers [10] considered that the potential of the nickel hydroxide electrode was held constant for states of charge between 10% and 55% by a surface layer of constant composition superimposed on a hysteric bulk reaction. In the present treatment the potential is considered to be fixed by pairs of co-existing solid solutions.

In a review of the nickel hydroxide electrode Milner and Thomas [1] have discussed the conclusions from a simple statistical mechanical treatment based on those of Bragg-Williams [21] and Guggenheim [19]. However, this model was invoked principally to explain the hysteresis between the charge and discharge processes by considering interactions between the oxidized and reduced species rather than as an explanation for the heterogeneity of the reversible potentials. Because the interaction model used by Milner and Thomas [1] is basically the same as that used in the present work, the equivalent criteria can be deduced regarding the conditions for phase separation. In the light of previous studies [11] it

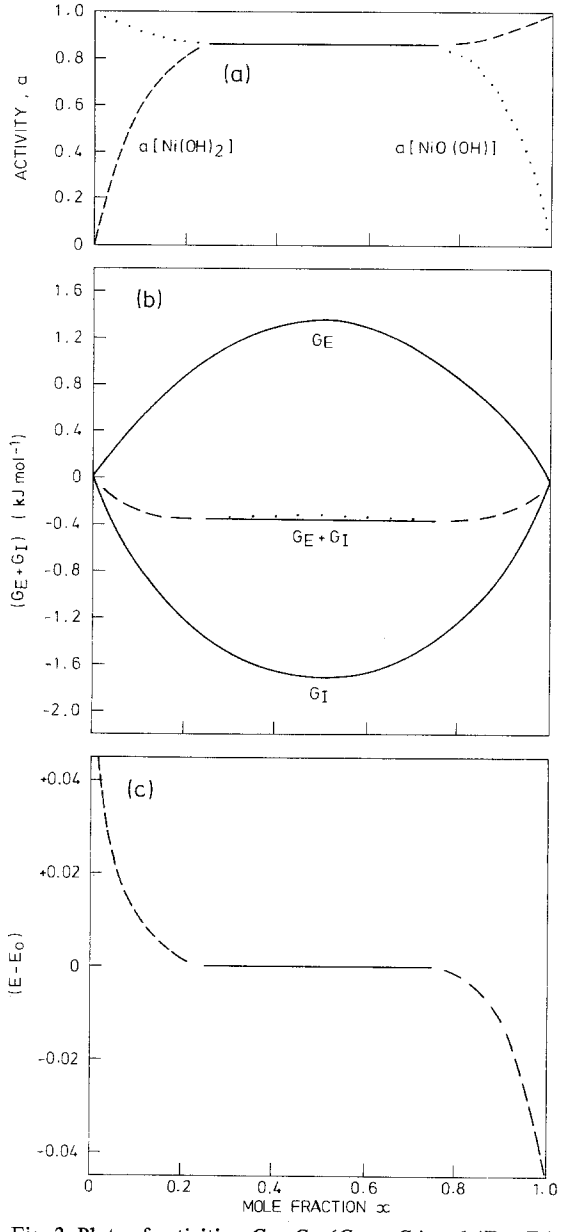


Fig. 3. Plots of activities, $G_E$, $G_I$, $(G_E + G_I)$ and $(E - E_0)$ against $x$ for a $\beta$-Ni(OH)$_2$/$\beta$-NiOOH electrode with $A/RT = 2{\cdot}2$.

appears that the apparent hysteresis between the charge and discharge reactions arises largely from the presence of a range of 'activated' and 'deactivated' oxidized and reduced phases having different $E_0$ values but clearly defined alkali and water contents.

## 5. Extension of the basic treatment

By using more complex expressions for $\gamma_y$ and $\gamma_z$, incorporating two interaction energy parameters $A_I$ and $B_I$ it is possible to account for the asymmetry in the $G_E$ function and also the potential–composition profile. Expressions for $\gamma_y$ and $\gamma_z$ derived from Van der Waal's theory have been proposed by Van Laar [18]

$$\ln \gamma_y = \frac{A_I x_z^2}{(x_z + B_I x_y)^2} \tag{38}$$

$$\ln \gamma_z = \frac{A_I B_I x_y^2}{(x_z + B_I x_y)^2} \tag{39}$$

The expressions used previously, Equations 9 and 10, are merely special cases of Equations 38 and 39 with $A_I = A/RT$ and $B_I = 1$ (taking note of Equation 8). The complete Nernst equation now becomes at constant pH:

$$E = \left(\frac{\mu_z^0 - \mu_y^0}{nF}\right) + \frac{RT}{nF}\left[\ln \frac{(1-x)}{x} + \frac{A_I(B_I x^2 - 1 + 2x - x^2)}{(1 - x + B_I x)^2}\right] \tag{40}$$

and

$$\frac{d(G_E + G_I)}{dx} = RT\left[\ln \frac{x}{(1-x)} - \frac{A_I(B_I x^2 - 1 + 2x - x^2)}{(1 - x + B_I x)^2}\right]. \tag{41}$$

On differentiation of Equation 41

$$\frac{d^2 G_M}{dx^2} = RT\left[\frac{1}{x(1-x)} - \frac{2A_I B_I}{(1 - x + B_I x)^3}\right]. \tag{42}$$

From the condition for phase separation as described previously and using Equations 19 and 20 in conjunction with Equations 38 and 39 the constants $B_I$ and $A_I$ can be evaluated thus:

$$B_I = \frac{2K(x_u + x_v - x_u x_v - 1) - (x_v + x_u + 2x_u x_v)}{(2x_u x_v) - K[2x_u x_v - (x_u + x_v)]} \tag{43}$$

where $$K = \ln\left(\frac{1 - x_u}{1 - x_v}\right) \Big/ \ln\left(\frac{x_u}{x_v}\right) \tag{44}$$

and

$$A_I = \frac{\ln (x_u/x_v)}{\dfrac{(1-x_v)^2}{[1+(B_I-1)x_v]^2} - \dfrac{(1-x_u)^2}{[1+(B_I-1)x_u]^2}} \quad (45)$$

The use of these more complex expressions with two adjustable parameters $A_I$ and $B_I$ is only justified if the compositions of the co-existing phases u and v are known with certainty. In the case of the nickel hydroxide system this is doubtful and Equations 40, 44 and 45 have little practical application. Nevertheless consideration of the effect of asymmetry on the $G_E$ function is of some significance because of its effect on $E_0$. The mathematical condition for phase separation arises whenever it is possible for a straight line to be drawn such that it is simultaneously tangential to the free energy curve at two points. As previously discussed for a symmetrical $G_E$ function the tangent line is horizontal at the minima such that $E = E_0$. However, for a non-symmetrical $G_E$ curve the tangent line is not horizontal and the points of contact are not at minima on the $(G_E + G_I)$ versus $x$ curve, hence $E \neq E_0$.

## 6. Application of the extended treatment to α-Ni(OH)$_2$/γ-NiOOH

In order to provide an illustration of the operation of the extended theory it is necessary to assign, albeit in a non-rigorous way, reasonable values for the composition of the phases u′ and v′. Previous equilibrium potential measurements have shown that the α-Ni(OH)$_2$/γ-NiOOH system gives a well-defined heterogeneous potential composition region like the corresponding β-phase system. As discussed in the previous paper [11] the γ-phase (phase V′) will be considered as being composed of $Ni^{2+}$ and $Ni^{4+}$ ions having an oxidation state of 3·67. Similarly, from the dependence of reversible potential with KOH activity, phase U′ can be deduced to have an oxidation state of 2·25. These oxidation states lead to values for $x_u$ and $x_v$ of 0·875 and 0·167 respectively. Fig. 4a shows the variation of the activities of the components Ni(OH)$_2$ and NiO$_2$ as a function of $x$ for the α/γ phase system. These values have been derived from Equations 38 and 39. Figs. 4b and c show the variation of $(G_E + G_I)$ and $E$ respectively as a function of $x$. The parameters $A_I = 2·37$ and

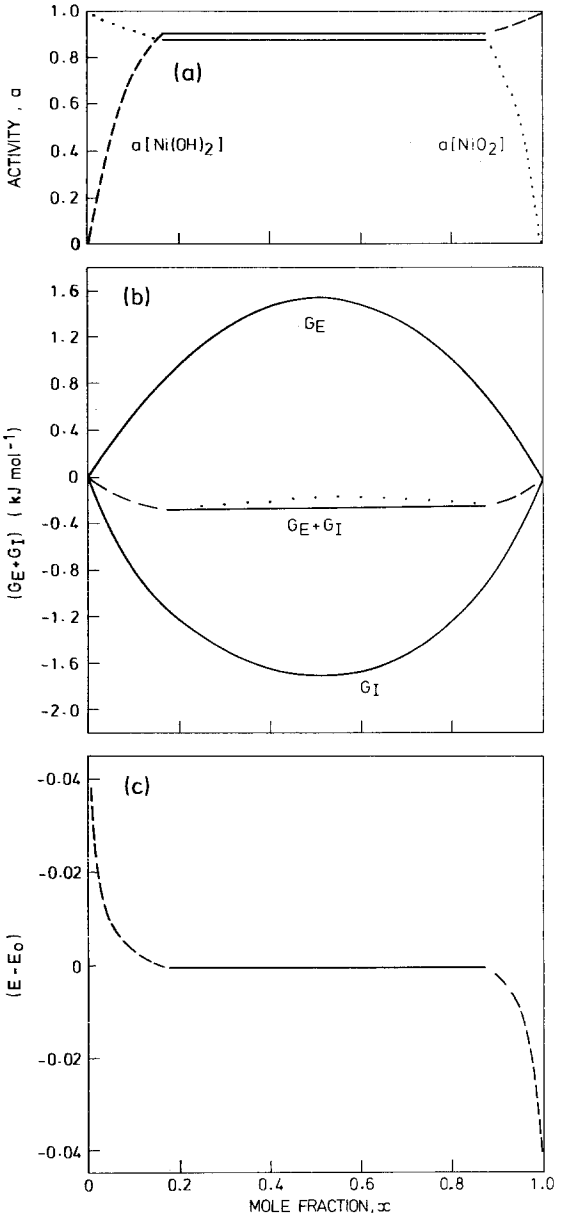


Fig. 4. Plots of activity, $G_E$, $G_I$, $(G_E + G_I)$ and $(E - E_0)$ against $x$ for an α-Ni(OH)$_2$/γ-NiOOH electrode with $A_I = 2·37$ and $B_I = 0·90$.

$B_I = 0·90$ were evaluated from the values for $x_u$ and $x_v$ using Equations 43 and 45. It is clear from Fig. 4c that moderate levels of asymmetry do not shift the horizontal potential region appreciably from $E_0$. The difference is of the order of 2 mV and is within the experimental error of the reversible potential measurements [11].

## 7. Model to describe the secondary discharge plateaux

In a previous paper [20] attention was drawn to the manifestation of a secondary discharge plateau at potentials 300 to 500 mV more cathodic than the normal operating potential. The development and maintenance of relatively high n-type semiconductivity in the initially low conductivity p-type $Ni(OH)_2$ starting material is crucial to the operation of the electrode. During discharge attempted removal of $Ni^{3+}$ defects in phase U can lead to premature failure [11, 20].

The active material present in a sintered plate electrode can be described in terms of a mixed p–n conductor in which n-type conductivity normally predominates. The current–voltage characteristics of such a material can be described by an equation of the type [22, 23]:

$$I = \frac{S}{L}\frac{RT}{F}\{\sigma_e^0[1 - \exp(-\eta F/RT)] + \sigma_h^0[\exp(\eta F/RT) - 1]\} \qquad (46)$$

where $I$ is current, $\eta$ potential, $\sigma_e^0$ and $\sigma_h^0$ the specific conductivity of electrons and holes and $R$, $T$ and $F$ have their previous significance. The quantity, $S$, is the area of contact between the active material and the current collector and $L$ is the distance from the current collector to the site of the reaction. In order to describe conductivity changes which take place during charging and discharging of a $\beta$-$Ni(OH)_2$/$\beta$-NiOOH electrode, it is necessary to have values for $\sigma_e^0$, $\sigma_h^0$, $S$ and $L$ as a function of oxidation state. None of these quantities are easily accessible and it is necessary to assume *a priori* that $\sigma_e^0$ and $\sigma_h^0$ vary with oxidation state as shown in Fig. 5. For the purpose of illustration $\sigma_h^0$ is considered to be invariant over the oxidation range 2·0–2·75 having the same value as for $\beta$-$Ni(OH)_2$, i.e. $10^{-14}$ $\Omega^{-1}$ $cm^{-1}$ [24]. It is assumed that $\sigma_e^0$ varies in proportion to the number of $Ni^{3+}$ ions injected into the $Ni(OH)_2$ lattice then:

$$\log \sigma_e^0 \propto \log\left(\frac{N}{N_0}\right) \qquad (47)$$

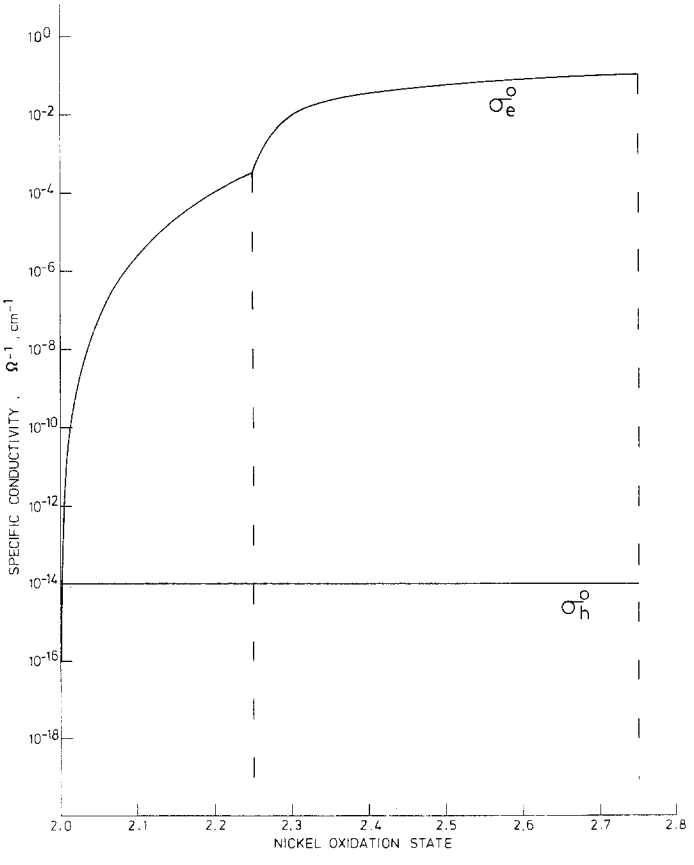


Fig. 5. Suggested electron and hole conductivities, $\sigma_e$ and $\sigma_h$, as a function of nickel oxidation state at 25° C.

where $N$ is the number of $Ni^{3+}$ ions per mole of active material and $N_0$ is Avogadro's number. According to Sagoyan *et al.* [24] the specific conductivity of the oxidized positive active material is in the range 0·01–0·15 $\Omega^{-1}$ $cm^{-1}$. In Fig. 5 the values for $\sigma_e^0$ for phase V ($Ni^{2\cdot75+}$) and phase U ($Ni^{2\cdot25+}$) are taken to be $10^{-1}$ and $3 \times 10^{-4}$ $\Omega^{-1}$ $cm^{-1}$ respectively. The discontinuity in conductivity when phase separation occurs at nickel oxidation states above 2·25 is simulated by assuming a parallel resistor network for components U and V. By using the values of $\sigma_e^0$ and $\sigma_h^0$ deduced for each oxidation state Fig. 6 may be constructed where the value of $S/L$ is fixed at $10^3$ cm. Because concentration polarization effects are small compared to the voltage changes caused by conductivity changes, the former can to a first approximation be disregarded from the present treatment.

During discharge, for values of $\eta > 0{\cdot}1$ V Equation 46 simplifies to:

$$I_{\text{discharge}} = \frac{S}{L}\frac{RT}{F}\left[\sigma_h^0 \exp(\eta F/RT) + \sigma_e^0\right]. \tag{48}$$

When $\sigma_h^0 \ll \sigma_e^0$, the current due to electrons reaches a plateau at a value of $(SRT/LF)\sigma_e^0$ until the hole current (which varies exponentially with $\eta$) takes over the conduction process. Fig. 6 shows the characteristic shape of the $\eta$ versus $I$ curves

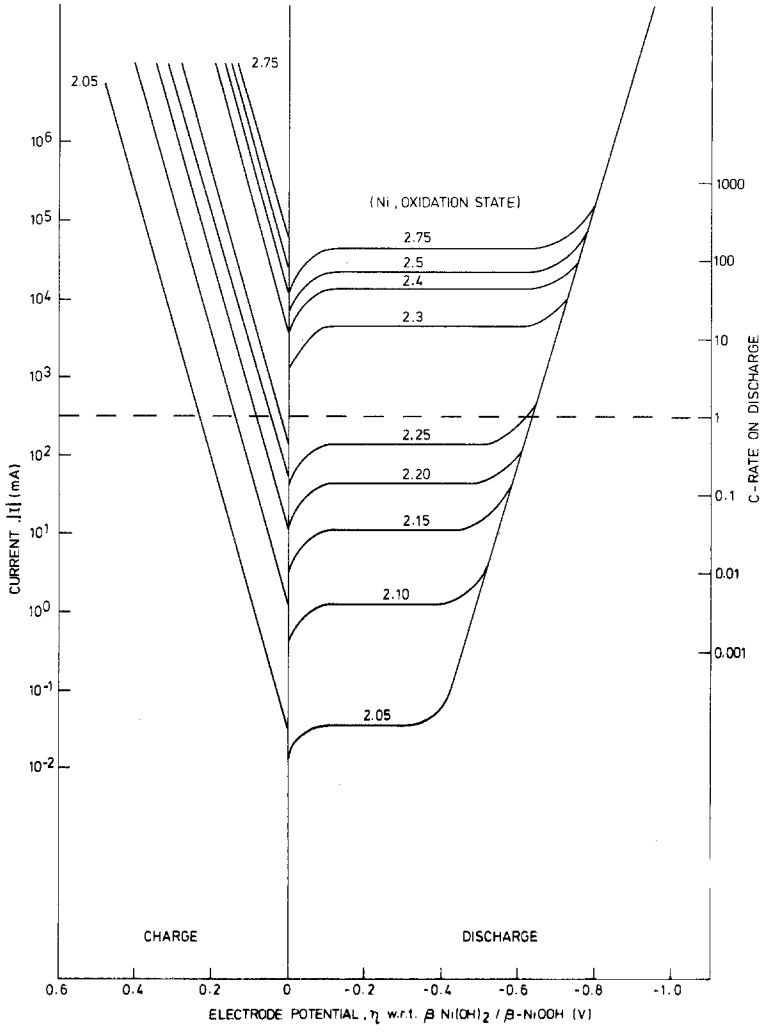


Fig. 6. Current $I$ versus potential $\eta$ plots for mixed electron–hole conductors. The diagram shows the anticipated behaviour for the $\beta$-$Ni(OH)_2$/$\beta$-NiOOH system at various nickel oxidation states indicated. Diagram refers to 1 g of $Ni(OH)_2$.

arising from the different conductivities of electrons and holes for the active material in various states of oxidation. Secondary discharge plateaux [20] arise in practice as a consequence of the discharge of active material having a nickel oxidation state below about 2·25 (phase U). The way in which these arise can be seen by examination of Fig. 6. At the $C/1$ discharge rate (dashed line in Fig. 6), it is clear for active material having an oxidation state $\geqslant 2{\cdot}3$ that discharge will take place near to the equilibrium potential value (i.e. $\eta = 0$ mV). On the other hand for oxidation states $\leqslant 2{\cdot}25$ discharge would be displaced cathodically by at least 640 mV. At high cathodic potentials the hydrogen evolution reaction dominates the shape of the real current–potential curves and is not considered in the present simplified model.

It is clear from Fig. 6 that the $S/L$ term is important with regard to establishing the minimum oxidation state which can be reached without manifestation of a secondary discharge step. For example, if $S/L$ were increased to $10^5$ the minimum oxidation state could be lowered to 2·1 before emergence of a secondary plateau. Thus by improving the integrity of the contact between the conducting matrix and the active material and by increasing the number of the peripheral contact points the 'residual capacity' can be minimized.

On charge no secondary step is expected because the charge carrier is predominantly the electron, i.e. $\sigma_e^0 \gg \sigma_h^0$. As a result Equation 46 simplifies to:

$$I_{\text{charge}} = \frac{SRT}{LF}\sigma_e^0 \exp(-\eta/RT). \qquad (49)$$

Curves of $\eta$ versus $I$ for the charge process at various states of oxidation are shown in Fig. 6. The behaviour of phase U is in some respects analogous to the rectifying action of heavily-doped semiconducting materials, i.e. small voltage drop when forward biased (charge direction) but a large voltage drop when reverse biased (discharge direction). The proposed model can be used to construct idealized curves for the discharge of a $\beta$-$Ni(OH)_2$/$\beta$-NiOOH electrode at various rates in the region of the secondary plateau as illustrated in Fig. 7. This diagram compares remarkably well with the general shape of the experimental curves observed previously [20].

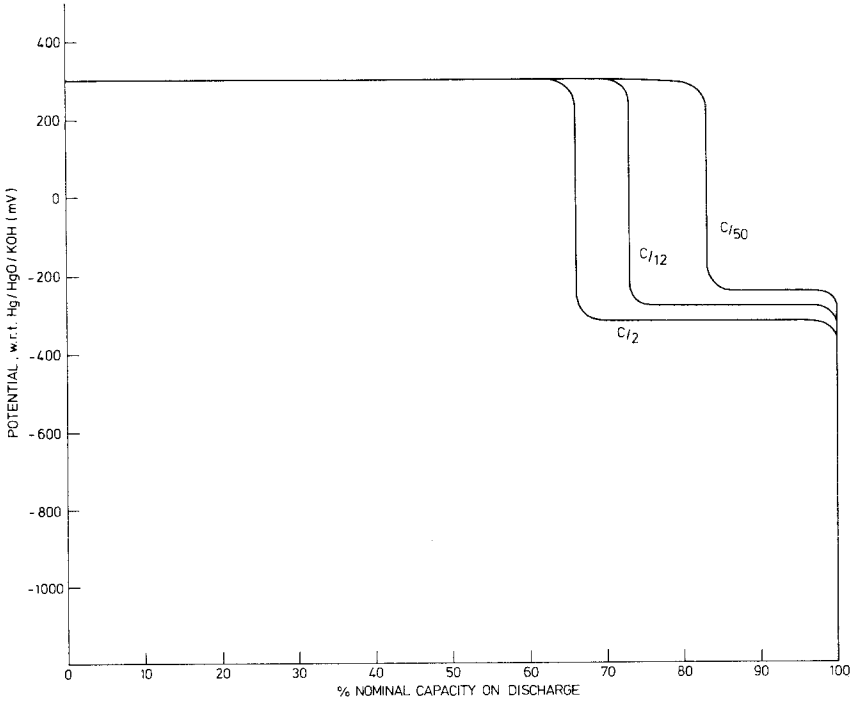


Fig. 7. Secondary discharge plateaux predicted from Fig. 6 for the $\beta$-NiOOH/$\beta$-$Ni(OH)_2$ electrode.

## 8. Estimation of free energy changes

Previous e.m.f. measurements [11] have shown that the $E_0$ values for various 'activated' and 'de-activated' nickel hydroxide/oxyhydroxide systems are as given below:

'activated' $\alpha$-phase ($U_1^*$)/$\gamma$-phase ($V_1^*$), $E_0^A$, 1·3179 V versus NHE

'de-activated' $\alpha$-phase ($U_1$)/$\gamma$-phase ($V_1^*$), $E_0^B$, 1·3663 V versus NHE

'activated', $\beta$-phase ($U^*$)/$\beta$-phase ($V^*$), $E_0^C$, 1·3688 V versus NHE

'de-activated', $\beta$-phase (U)/$\beta$-phase ($V^*$), $E_0^D$, 1·3961 V versus NHE.

The total free energy of mixing, $G_M$ is given by Equations 11 and 12. However, because the free energy of reaction, $G_R$ is of the order of $-500\,kJ\,mole^{-1}$ and the other terms are only about $1\,kJ\,mole^{-1}$ the free energy varies linearly with the mole fraction of nickel hydroxide, $x$, to a very close approximation. Thus by knowing the standard free energies of formation of $\beta$ and $\alpha$-$Ni(OH)_2$ together with the oxidation states of the co-existing phases, Fig. 8 can be constructed. The standard free energy of formation of $\beta$-$Ni(OH)_2$ is taken as $-452{\cdot}7\,kJ\,mole^{-1}$ [25], whilst Bode [2] has shown the free energy difference between $\alpha$ and $\beta$-$Ni(OH)_2$ to be $14{\cdot}2\,kJ\,mole^{-1}$. The oxidation state of phases U, $U^*$, $U_1$ and $U_1^*$ is taken to be 2·25 whilst that of $V^*$ is 2·75 and of $V_1^*$, 3·67.

It is of interest to compare our estimates of the free energies for phases $V^*$ and $V_1^*$ (i.e. $\beta$-NiOOH and $\gamma$-NiOOH) of $-553{\cdot}7$ and $-679{\cdot}3\,kJ\,mole^{-1}$

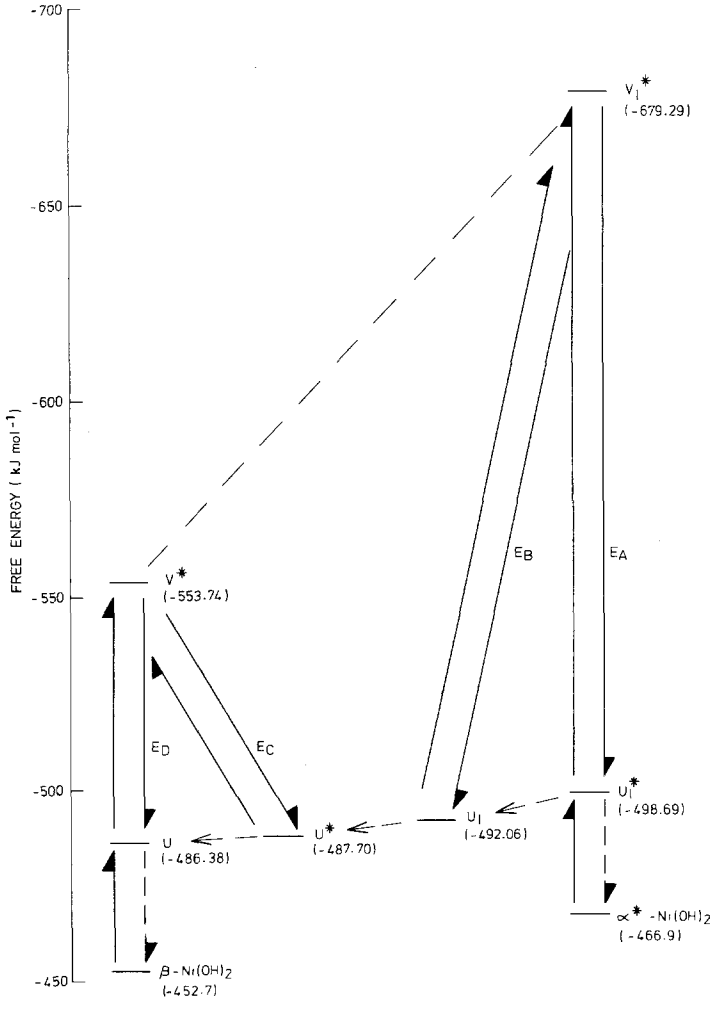


Fig. 8. Free-energy level diagram for the various nickel hydroxide–oxyhydroxide phases. Asterisks denote 'activated' phases.

with those of other workers. Values for β-NiOOH have been given as $-565{\cdot}2\ \text{kJ mole}^{-1}$ by Hodge *et al.* [26], $-707{\cdot}94\ \text{kJ mole}^{-1}$ by Pourbaix [27] and $-542{\cdot}61\ \text{kJ mole}^{-1}$ by Latimer [25]. Values for the γ-phase have not been reported previously in the literature. Clearly the values obtained in this investigation for the β-phase are in reasonable agreement with those generally found in the literature in spite of the fact that mixed β/γ phases are likely to have been present in the earlier work.

In deriving Fig. 8 it has been assumed that electrochemical oxidation always leads to an 'activated' product i.e. $V^*$ or $V_1^*$. Some justification for this approach can be found from the observation that the $E_0'$ values decrease if the charged active material is allowed to age at an elevated temperature [11]. Thus it is highly likely that the energy level diagram is more complex than that given in Fig. 8 because 'de-activated' oxidized phases V and $V_1$ would also need to be considered. Information is not available for these materials at present.

It should be emphasized, as discussed previously [11], that an extensive range of 'activated' and 'de-activated' reduced phases are likely to exist leading to a band of free energy values rather than discrete absolute values.

## 9. Influence of dissociation of the oxidized and/or reduced species on the equilibrium potentials

In Section 3 equations were derived which tacitly assumed that the oxidized and reduced species were always undissociated in character. Evidence has been provided recently to indicate the possibility of dissociation in the γ-$MnO_2$/MnOOH system [29] and in the hydrogen tungsten bronzes [30, 31] $WO_3/H_xWO_3$. It was considered important therefore to extend this concept to the β-$Ni(OH)_2$/β-NiOOH system. The influence of ionization is revealed from a consideration of the limiting slopes for *dilute* solid solutions of the oxidized and reduced species. Under these circumstances the activity coefficients can be regarded as approaching a constant value. In order to establish viable equations some care is needed in deciding upon the dissociation mode for the components. Since the proton is the only species which has significant mobility at room temperature it is reasonable, by anology [29, 30] with $WO_3/H_xWO_3$, to postulate simple binary ionization processes as follows:

$$Ni^{II}(OH)_2 \rightleftharpoons Ni^{II}(OH)O^- + H^+ \qquad (50)$$

$$Ni^{III}O(OH) \rightleftharpoons Ni^{III}OO^- + H^+. \qquad (51)$$

These in turn can be shown to give rise to the following Nernst equations (at constant pH).

### 9.1. *Case 1*

When both $Ni(OH)_2$ and NiOOH are associated then the potential is given by:

$$(E - E_0) = \frac{RT}{nF} \ln \frac{\gamma_z}{\gamma_y} + \frac{RT}{nF} \ln \frac{(1-x)}{x}. \qquad (52)$$

When $x \to 1$ or 0 the limiting slope for $(E - E_0)$ versus $\log (1-x)/x$ is 59 mV/decade, since the terms incorporating the activity coefficients ($\gamma_z$ and $\gamma_y$) tend towards a constant value. Equation 52 is merely a different form of Equation 2 describing the behaviour for an infinitely dilute solid solution showing ideal behaviour.

### 9.2. *Case 2*

If NiOOH is considered to be a completely dissociated solute in associated $Ni(OH)_2$ solvent then the potential can be shown to be given by:

$$(E - E_0) = \frac{RT}{nF} \ln \frac{(\gamma_z^{\pm})^2}{\gamma_y} + \frac{RT}{nF} \ln \frac{(1-x)^2}{x(2-x)}. \qquad (53)$$

If $x \to 0$ this would give a limiting slope for a plot of $(E - E_0)$ versus $\log (1-x)/x$ of 59 mV/decade and for $x \to 1$ of 118 mV/decade.

### 9.3. *Case 3*

If NiOOH is associated and the $Ni(OH)_2$ completely dissociated then the potentials are given by

$$(E - E_0) = \frac{RT}{nF} \ln \frac{\gamma_z}{(\gamma_y^{\pm})^2} + \frac{RT}{nF} \ln \frac{(1-x^2)}{x^2}. \qquad (54)$$

This system behaves as the inverse of case 2, namely that the limiting slope for a plot of $(E - E_0)$ versus $\log (1-x)/x$ tends as $x \to 0$ to 118 mV/decade and as $x \to 1$ to 59 mV/decade.

9.4. *Case 4*

If both $Ni(OH)_2$ and NiOOH are completely dissociated then the potentials are given by

$$(E-E_0) = \frac{RT}{nF}\ln\frac{(\gamma_z^{\pm})^2}{(\gamma_y^{\pm})^2} + \frac{RT}{nF}\ln\frac{(1-x)^2}{x^2} \tag{55}$$

Plots of $(E-E_0)$ versus $\log(1-x)/x$ always tend to 118 mV when $x \to 1$ or 0.

The only experimental data available relates to nickel hydroxide at low states of charge i.e. where $x \to 1$. In practice valence states above $Ni^{2\cdot75}$ in the $\beta$-phase system are difficult to study because of contamination [11] by the $\gamma$-phase. From the data of Conway and Gileadi [10] it is clear that as $x \to 1$ a limiting slope of ~ 59 mV/decade is indicated, consequently cases 1 or 3 could apply. In view of the likelihood that neither NiOOH or $Ni(OH)_2$ are strongly acidic an associated model case 1 is preferred. Chemical evidence suggests that $Ni(OH)_2$ is distinctly basic in character and as the acidity of the proton generally increases with increasing state of oxidation it is unlikely that NiOOH in dilute solid solution is less acidic than $Ni(OH)_2$. Clearly the $\beta$-$Ni(OH)_2$/$\beta$-NiOOH system differs from those of $\gamma$-$MnO_2$/MnOOH [29] and $WO_3/H_xWO_3$ [30, 31] where dissociation is manifest. The $\beta$-$Ni(OH)_2$/$\beta$-NiOOH couple resembles more the undissociated behaviour displayed by the $\beta$-$MnO_2$/MnOOH system [29]. There is a greater possibility that the $\alpha$-$Ni(OH)_2$/$\gamma$-NiOOH system may show the presence of dissociation. Unfortunately there are no experimental data available which have bearing on the subject. Again because of a limit in the oxidation state for the $\gamma$-phase, information relating to cases where $x \to 0$ is inaccessible. However, it might be possible to distinguish between cases 1 and 2, using data at low states of charge where $x \to 1$.

In the case of the $\beta$-$Ni(OH)_2$/$\beta$-NiOOH cathode the concept of co-existing solid solutions is of prime importance for establishing the source of the reversible potential over the greater part of the oxidation/reduction range. Accordingly the influence of dissociation when marked deviations from ideality clearly exist is only of secondary importance. It is interesting to note that an equation of the form of Equation 56 derived from statistical thermodynamics [31]

$$E = E_0 + \frac{RT}{nF}\psi\ln\frac{(1-x)}{x} + \frac{A}{nF}(2x-1) \tag{56}$$

can be used to describe the behaviour of non-ideal, ionic solid solutions where the minority (reduced species) is dissociated in the host (oxidized) lattice. If the proton and electron pair have close spatial correlation [31] then $\psi = 1$ and Equation 56 relates to undissociated oxidized and reduced phases and is identical to Equation 15 previously derived. If, however, the proton and electron do not have close spatial correlation then $\psi = 2$ and the reduced phase can be considered as dissociated in the oxidized phase (case 3 behaviour).

It may be noted that the thermodynamic criterion for dissociation of the proton in the oxidized or reduced phase may not necessarily be a general guide to cathode suitability. Kinetic factors concerning the mode in which the proton–electron pair move are of obvious importance. Clearly the modes of proton transport in $\gamma$-$MnO_2$/MnOOH and $\beta$-$Ni(OH)_2$/NiOOH are likely to be different because both materials function as high rate cathode materials. It is interesting to note that the $Ni(OH)_2$/NiOOH electrode shows a similarity to the $\alpha/\beta$ palladium hydride reference electrode [28] which also utilizes co-existing phases to fix the equilibrium potential.

**Acknowledgement**

Thanks are due to Dr Armitage of Leicester Polytechnic for helpful suggestions and to the Directors of Berec Group Limited for permission to publish this work.

**References**

[1] P. C. Milner and U. B. Thomas in 'Advances in Electrochemistry and Electrochemical Engineering' Vol. 5, Interscience, New York (1967) p. 20.
[2] H. Bode, K. Dehmelt and J. Witte, *Electrochim. Acta* **11** (1966) 1079.
[3] *Idem, Z. Anorg. Chem.* **366** (1969) 1.
[4] O. Glemser and J. Einerhand, *Z. Anorg. Chem.* **261** (1950) 26.
[5] G. W. D. Briggs and W. F. K. Wynne-Jones *Trans. Faraday Soc.* **52** (1956) 1260.
[6] *Idem, Electrochim. Acta* **7** (1962) 241.

[7] E. M. Kuchinskii and B. V. Ershler, *Zh. Fiz. Khim.* **20** (1946) 539.
[8] G. W. D. Briggs and M. Fleischmann, *Trans. Faraday Soc.* 67 (1971) 2397.
[9] K. Takahashi, S. Yoshizawa and A. Kozawa, 'Electrochemistry of Manganese Dioxide and Manganese Dioxide Batteries in Japan' **2** (1971) 51, US Branch Office, Electrochem Soc., Japan.
[10] B. E. Conway and E. Gileadi, *Canad. J. Chem* **40** (1962) 1933.
[11] R. Barnard, C. F. Randell and F. L. Tye, *J. Appl. Electrochem.*
[12] F. P. Kober, *J. Electrochem. Soc.* **112** (1965) 1066.
[13] *Idem, ibid* **114** (1967) 215.
[14] I. K. Kuchkaeva, I. S. Shamina, P. N. Bityutskii and L. A. Chetovskaya, *Zhur. Priklad. Spektroskopii* **17** (1972) 921.
[15] R. Barnard and G. T. Crickmore, published results.
[16] I. S. Shamina, O. S. Malandin, S. M. Rakhovskaya and L. A. Vereshchagina *Electrokhim.* **10** (1974) 1571.
[17] S. Atlung, *$MnO_2$ Symposium 1* Cleveland Ohio, JECS (1975) p. 47.
[18] J. H. Hildebrand and R. L. Scott, 'The Solubility of Non-Electrolytes', Reinhold, New York (1948).
[19] E. A. Guggenheim, 'Mixtures' Oxford, London (1952).
[20] R. Barnard, G. T. Crickmore, J. A. Lee and F. L. Tye, *J. Appl. Electrochem.*
[21] W. L. Bragg and E. J. Williams, *Proc. Roy. Soc. Serr.* **A145** (1939) 699.
[22] A. V. Joshi, 'Fast Ion Transport in Solids' Edited by Van Gool, North Holland Publishing Co. p. 173.
[23] J. B. Wagner, 'Fast Ion Transport in Solids' Edited by Van Gool, North Holland Publishing Co. p. 489.
[24] L. N. Sagoyan, Yu. M. Gulyamov, P. Z. Barsukov and V. E. Dmitrenko, *28th I.S.E. Meeting* Bulgaria (1977) Extended Abstract 82.
[25] W. M. Latimer, 'The Oxidation States of the Elements and their Potentials in Aqueous Solutions' Prentice Hall, New Jersey (1952).
[26] B. J. R. Hodge, R. Bonnaterre and F. Putois, 'Power Sources 5' edited by D. H. Collins, Academic Press, New York (1975) p. 219.
[27] M. Pourbaix, 'Atlas d'Equilibres Electrochimiques' Gauthier-Villars (1963).
[28] F. A. Lewis, 'The Palladium/Hydrogen System', Academic Press, London (1967).
[29] F. L. Tye, *Electrochim. Acta.* **21** (1976) 415.
[30] M. L. Hitchman, *J. Electroanalyt. Chem.* 85 (1977) 135.
[31] R. S. Crandall, P. J. Wojtowicz and B. W. Faughnan, *Sol. State Comm.*, **18** (1976) 1409.